PHYSICAL REVIEW B **79**, 100105(R) (2009)

Nature of the ferroelectric phase transition in multiferroic $BiFeO_3$ from first principles

Igor A. Kornev[1] and L. Bellaiche[2]
[1]*Laboratoire SPMS, UMR 8580 du CNRS, Ecole Centrale Paris, 92295 Chatenay-Malabry, France*
[2]*Department of Physics, University of Arkansas, Fayetteville, Arkansas 72701, USA*
(Received 16 January 2009; published 18 March 2009)

A first-principles-based scheme is used to investigate the nature of the ferroelectric phase transition in the multiferroic $BiFeO_3$. This transition possesses several order parameters (that are components of the polarization and of the tilting of oxygen octahedra) *with none of them being primary* and is solely driven by the *collaborative coupling* between the polarization and the other order parameters. This phase transition is therefore neither proper nor improper but rather can be regarded as a special trigger-type transition. Our atomistic simulations also reveal the precise origins and mechanisms of this trigger-type phase transition.

DOI: 10.1103/PhysRevB.79.100105 PACS number(s): 77.80.Bh, 64.60.−i, 75.40.Mg, 77.22.Ch

Multiferroics form a class of materials that can simultaneously exhibit polarization and magnetic ordering.[1] They are of high current interest mostly because of the cross coupling between these ferroelectric (FE) and magnetic order parameters (OPs)—see, e.g., Refs. 2 and 3 and references therein. $BiFeO_3$ (BFO) is often referred to as "the holy grail of the multiferroics"[4] because it possesses both ferroelectricity and magnetic ordering *at room temperature*—as a consequence of a paraelectric-to-FE transition occurring around (the Curie temperature) T_C=1083–1103 K (Refs. 5 and 6) and of a cycloidal spin structure superimposed on a *G*-type antiferromagnetism[7] below T_N=625–643 K.[5,8] Puzzling features have been reported in BFO around its Curie temperature, including the complete suppression of the Raman spectra[9] and a striking deviation of the dielectric response from a Curie-Weiss behavior[10] above T_C,[11] as well as the FE transition being of first order with no group-subgroup relation between the paraelectric and polar phases.[11] Such anomalous effects seem to imply that BFO is not a "proper" FE and have led its FE phase transition to be denoted as being of the "improper" type.[11,12] It is important to recall that the primary OP (an OP is called primary if it energetically drives the phase transition[13]) of a proper FE is the spontaneous polarization itself, while the polarization is only a *secondary* OP in improper FEs.[14] In other words, the primary OP of improper FEs is another physical quantity [such as the magnetic moments in perovskite rare-earth manganites[15–17] and some tilting of the AlO_4 oxygen octahedra in $BaAl_2O_4$ (Ref. 18)], with the coupling between this other quantity and the polarization being responsible for the appearance of the polarization below T_C. It is obviously of high importance to know the nature of the FE transition in BFO and the mechanisms governing it.

The aim of this Rapid Communication is to revisit the nature of the FE phase transition of BFO via the use of a first-principles-based scheme. We found that such transition is indeed not proper, but—surprisingly—it is not improper either. More precisely, it does *not* possess any primary OP belonging to a single irreducible representation and is rather solely driven by the *collaborative* coupling between the polarization and the oxygen octahedra tilting.[19] It is a special trigger-type transition.[20] Our simulations also reveal the precise origins and mechanisms of this trigger-type transition.

The total internal energy, E_{tot}, of BFO is provided by the effective Hamiltonian approach of Ref. 11. It possesses four degrees of freedom: (i) the strain tensor, $\{\eta\}$ (Ref. 21); (ii) the magnetic dipole moment, $\mathbf{m}_i$, centered on the Fe site i (Ref. 11); (iii) the local FE soft modes in unit cells i, $\{\mathbf{u}_i\}$ (which are directly proportional to the electrical dipole centered on those sites[21]); and (iv) the $\{\omega_i\}$ vectors that characterize the direction and magnitude of the antiferrodistortive (AFD) motions in unit cell i (Ref. 22); E_{tot} consists of 13 different parts:[11,21,22] an elastic energy (quadratic in η); the exchange interactions associated with magnetic moments (quadratic in $\mathbf{m}_i$); a self-energy for FE degrees of freedom (quartic in $\mathbf{u}_i$); a long-range electric dipole-dipole interaction (quadratic in $\mathbf{u}_i$); a short-range interaction between local soft modes (quadratic in $\mathbf{u}_i$); the self-energy associated with AFD motions (quartic in ω_i); the short-range interaction energy between AFD degrees of freedom (quadratic in ω_i); an interaction between strain and magnetism (linear in η and quadratic in $\mathbf{m}_i$); an interaction energy between strain and local modes (linear in η and quadratic in $\mathbf{u}_i$); an interaction between strain and AFD degrees of freedom (linear in η and quadratic in ω_i); an interaction term between magnetism and ferroelectricity (quadratic in both $\mathbf{m}_i$ and $\mathbf{u}_i$); an interaction between magnetism and AFD motions (quadratic in both $\mathbf{m}_i$ and ω_i); and the $E_{\text{FE-AFD}}$ interaction energy between local soft modes and AFD motions, which takes the following expression (according to symmetry considerations with respect to a cubic state):

$$\begin{aligned} E_{\text{FE-AFD}}(\{\mathbf{u}_i\},\{\omega_i\}) = \sum_i \{ & D_{xxxx}[u_{i,x}^2\omega_{i,x}^2 + u_{i,y}^2\omega_{i,y}^2 + u_{i,z}^2\omega_{i,z}^2] \\ & + D_{xxyy}[u_{i,x}^2(\omega_{i,y}^2 + \omega_{i,z}^2) + u_{i,y}^2(\omega_{i,z}^2 + \omega_{i,x}^2) \\ & + u_{i,z}^2(\omega_{i,x}^2 + \omega_{i,y}^2)] + D_{xyxy}[u_{i,x}u_{i,y}\omega_{i,x}\omega_{i,y} \\ & + u_{i,y}u_{i,z}\omega_{i,y}\omega_{i,z} + u_{i,z}u_{i,x}\omega_{i,z}\omega_{i,x}]\}, \end{aligned} \quad (1)$$

where the sum over i runs over all unit cells and where the x, y, and z subscripts refer to Cartesian coordinates along the [100], [010], and [001] pseudocubic directions, respectively. D_{xxxx}, D_{xxyy}, and D_{xyxy} are parameters of this expansion. The first-principles-based parameters of E_{tot} are those of Ref. 11 and yield an excellent agreement with measurements for the Néel and Curie temperatures (around 635 and 1075 K, respectively), as well as for the magnetoelectric coefficients.[11] Technically, E_{tot} is used in Monte Carlo (MC) simulations to compute finite-temperature properties of BFO. We use 14

$\times 14 \times 14$ supercells (13 720 atoms) and 400 000 MC sweeps to get converged results. Relevant outputs are the **u** supercell average of the local mode vectors $\{\mathbf{u}_i\}$ and the $\omega_{\mathbf{R}}$ vector defined as $\omega_{\mathbf{R}}=\frac{1}{N}\Sigma_i\omega_i(-1)^{n_x(i)+n_y(i)+n_z(i)}$—where the sum runs over the unit cells and where $n_x(i)$, $n_y(i)$, and $n_z(i)$ are integers locating the cell i. A nonvanishing **u** indicates ferroelectricity, while a nonzero $\omega_{\mathbf{R}}$ characterizes AFD motions associated with the R point of the cubic first Brillouin zone, respectively. We also compute the following quantities:

$$\chi_{\alpha\alpha}=\frac{(NZ^*)^2}{V\epsilon_o k_B T}[\langle u_\alpha^2\rangle-\langle u_\alpha\rangle^2],$$

$$\chi_{\alpha\alpha}^{\omega_R}=\frac{N^2}{Vk_BT}[\langle \omega_{R,\alpha}^2\rangle-\langle \omega_{R,\alpha}\rangle^2], \quad (2)$$

where "$\langle\ \rangle$" denotes statistical averages and where u_α and $\omega_{R,\alpha}$ are the α component of **u** and $\omega_{\mathbf{R}}$, respectively. N is the number of sites in the supercell, while V is its volume. Z^* is the Born effective charge associated with the local mode, k_B is the Boltzmann constant, and ϵ_o is the permittivity of vacuum. $\chi_{\alpha\alpha}$ are the diagonal elements of the dielectric susceptibility tensor,[23,24] while $\chi_{\alpha\alpha}^{\omega_R}$ is the staggered susceptibility[25] associated with $\omega_{R,\alpha}$.

Figure 1(a) shows the predicted x-, y-, and z-Cartesian coordinates ($\langle u_1\rangle$, $\langle u_2\rangle$, and $\langle u_3\rangle$) of $\langle\mathbf{u}\rangle$ in BFO, while Fig. 1(b) displays $\langle\omega\rangle_R$ (with $\langle\omega_1\rangle_R$, $\langle\omega_2\rangle_R$, and $\langle\omega_3\rangle_R$ denoting the x-, y-, and z-Cartesian coordinates of $\langle\omega\rangle_R$), and Fig. 1(c) reports the susceptibilities. Figures 1(a) and 1(b) indicate that, as consistent with experiments (see Ref. 9 and references therein), our numerical scheme predicts a $R3c$ *ground state* that exhibits a polarization pointing along the [111] direction (since $\langle u_1\rangle=\langle u_2\rangle=\langle u_3\rangle\neq 0$ at the lowest temperatures) and a tilting of the oxygen octahedra about the [111] axis (since $\langle\omega_1\rangle_R=\langle\omega_2\rangle_R=\langle\omega_3\rangle_R\neq 0$ at the lowest temperatures). Figure 1 also indicates a *first-order* FE-to-paraelectric transition from a rhombohedral $R3c$ phase to a tetragonal $I4/mcm$ state that solely exhibits AFD motions about the [001] axis, about $T_C\simeq 1075$ K as indicated by the nonzero value of $\langle\omega_3\rangle_R$ above $\simeq 1075$ K in Fig. 1(b) and the vanishing of $\langle\mathbf{u}\rangle$ via the jump seen in Fig. 1(a) around 1075 K. Figure 1(a) thus reveals that $\langle u_1\rangle$, $\langle u_2\rangle$, $\langle u_3\rangle$, $\langle\omega_1\rangle_R$, and $\langle\omega_2\rangle_R$ are the OPs of this FE transition. The $I4/mcm$ phase exists up to a temperature, $T_{\mathrm{AFD}}\simeq 1440$ K, before transforming to the cubic $Pm\bar{3}m$ state. Figure 1(c) further shows that the $\chi_{\alpha\alpha}$'s dramatically deviate from a Curie-Weiss law[10] just above T_C and up to T_{AFD} (that is within the tetragonal $I4/mcm$ phase): they *slightly decrease* (rather than rapidly increase) as the temperature is lowered from 1440 to 1075 K. Hence, there is no softening of the phonon mode associated with the polarization when approaching T_C from above, unlike in *proper* FEs. Such dielectric anomaly has been reported for *improper* FEs (Ref. 14) for which the primary OP is not the polarization. One natural suspect for the primary OP is the tilting of the oxygen octahedra. However, the inset of Fig. 1(c) tells us that the $\chi_{\alpha\alpha}^{\omega_R}$ coefficients all *decrease* as the temperature is decreased from T_{AFD} down to T_C. Therefore, the phonon mode associated with the AFD motions does not soften when approaching the $R3c$–to–$I4/mcm$ transition from above, which implies that the tilting of the oxygen octahedra is not the primary OP of the FE transition either. The other possible candidates for this primary OP are the (antiferro)magnetic vector or strain since our numerical scheme only contains these two latter degrees of freedom, in addition to the FE and AFD motions. However, the features of Fig. 1 all qualitatively remain when turning *off* the magnetic dipoles and the strain variables in our simulations. As a result, we can undoubtedly conclude that the FE transition of BFO does not have any primary OP or, equivalently, that BFO is neither a proper nor an improper FE! (Note also that the "normal" evolution of the polarization below T_C depicted

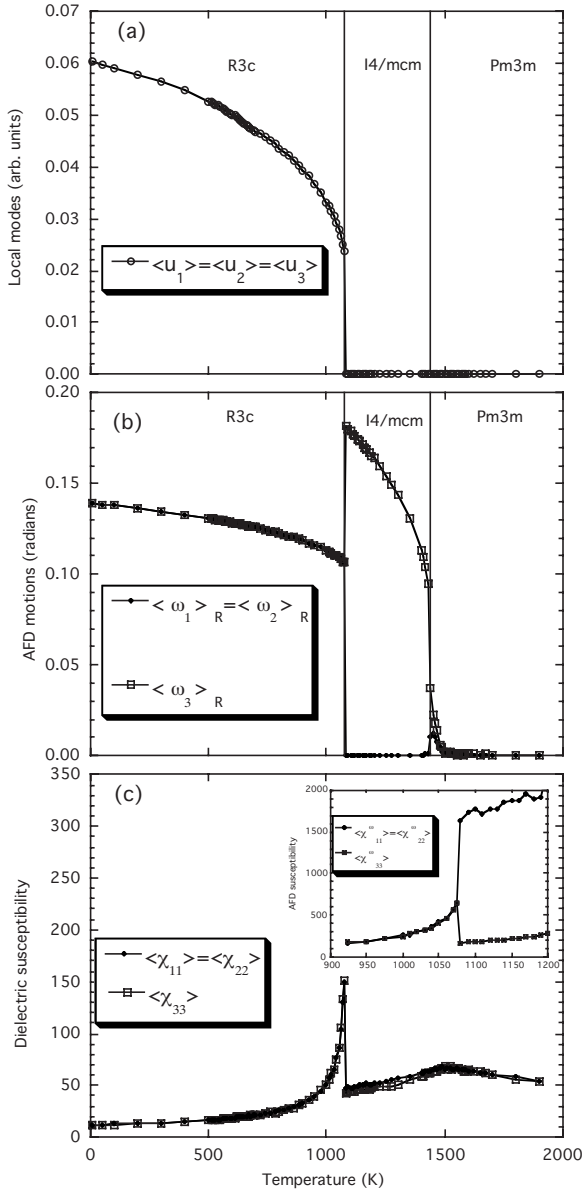

FIG. 1. Supercell average $\langle\mathbf{u}\rangle$ of the local mode vectors [panel (a)], AFD-related $\langle\omega\rangle_R$ quantity [panel (b)], and $\chi_{\alpha\alpha}$ dielectric susceptibilities [panel (c)] as a function of temperature in BFO and as predicted by the scheme of Ref. 11. χ_{11} is identical to χ_{22} and is thus not shown for clarity. The inset displays $\chi_{33}^{\omega_R}$ and $\chi_{22}^{\omega_R}$ (with this latter quantity being equal to $\chi_{11}^{\omega_R}$) around T_C in arbitrary units.

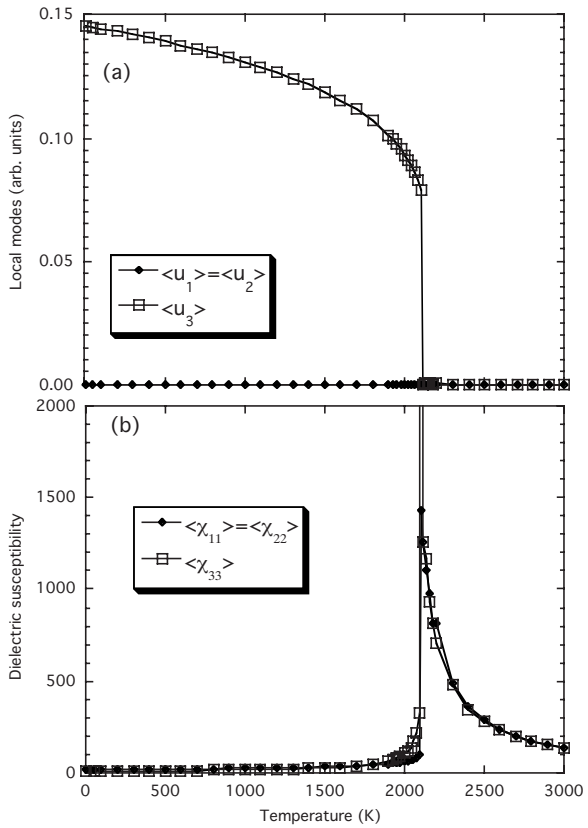

FIG. 2. Supercell average $\langle \mathbf{u} \rangle$ of the local mode vectors [panel (a)] and $\chi_{\alpha\alpha}$ dielectric susceptibilities [panel (b)] as a function of temperature in BFO and as predicted by the scheme of Ref. 11 in which the AFD and magnetic degrees of freedom are turned off.

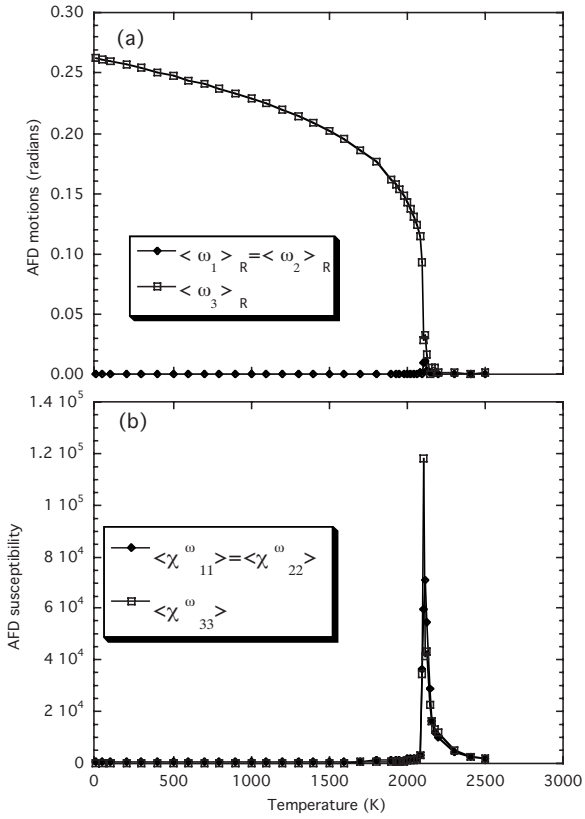

FIG. 3. Supercell average of the AFD-related $\langle \omega \rangle_R$ quantity [panel (a)] and AFD staggered susceptibilities [panel (b)] as a function of temperature in BFO and as predicted by the scheme of Ref. 11 in which the FE and magnetic degrees of freedom are turned off.

in Fig. 1(a) is not what is expected for a usual improper FE.[14])

To determine the nature of this transition, we performed two additional kinds of simulations. In the first type whose results are shown in Fig. 2, the AFD motions, as well as the magnetic dipole moments, are forced to vanish, implying that we only investigate here the sole effect of FE and its coupling with strain on properties. On the contrary, the FE degrees of freedom, and still the magnetic dipole moments, are kept to zero in the second kind of simulations. This second type, whose results are depicted in Fig. 3, thus corresponds to the case for which only AFD motions and strains can appear in BFO. One can see that *neglecting the AFD degrees of freedom* leads to a ground state that is FE tetragonal ($P4mm$) with a polarization pointing along the $\langle 001 \rangle$ direction and to only one transition from $P4mm$–to–$Pm\bar{3}m$ when increasing the temperature from 0 K. This latter FE transition occurs at a very high temperature (i.e., $\simeq$2100 K), is of first order [see the jump in $\langle u_3 \rangle$ in Fig. 2(a)], and is proper since the dielectric susceptibility now adopts a Curie-Weiss behavior above T_C [see Fig. 2(b)]. Moreover, when *neglecting the FE variables*, the ground state has the $I4/mcm$ space group [see Fig. 3(a)] and only one transition from $I4/mcm$–to–$Pm\bar{3}m$ occurs at a very high temperature (around 2100 K). As shown by Fig. 3(b), the staggered susceptibilities also behave in a normal, Curie-Weiss fashion above that transition. Comparing Figs. 2 and 3 with Fig. 1 and knowing the sign and magnitude of the coefficients of Eq. (1) determined from first principles [that is, D_{xxxx} and D_{xxyy} being strongly positive while D_{xyxy} being even larger but negative] shed some light on the properties of BFO displayed in Figs. 1. For instance, at high temperature, the FE and AFD motions fight against each other since they do not want to coexist in a tetragonal phase (in which $\mathbf{u}$ and $\boldsymbol{\omega}_\mathbf{R}$ would both lie along the same $\langle 001 \rangle$ direction) because of the positive, large D_{xxxx}; this despite the fact that they *separately* desire to generate a tetragonal state below 2100 K [see Figs. 2(a) and 3(a)].[26] Such fight leads to the vanishing of the polarization above T_C=1075 K and to the sole appearance of the oxygen octahedra tilting (within the $I4/mcm$ phase) between T_C and T_{AFD}=1440 K. For lower temperature, BFO exhibits the $R3c$ phase as a consequence that both FE and AFD motions possess strong instabilities (see Figs. 2 and 3) and that FE and AFD degrees of freedom can coexist in a rhombohedral state because of the negative, large D_{xyxy}. Moreover, we conducted further simulations, around T_C, in which an electric field is applied to directly influence the polarization and determine its effect on the AFD degrees of freedom, as well as other computations in which the conjugate, staggered field[25] of $\boldsymbol{\omega}_\mathbf{R}$ is applied to directly influence the AFD motions and follow its effect on the polarization. We found that any *specific value* of $\langle u_1 \rangle = \langle u_2 \rangle = \langle u_3 \rangle$ is associated with a *specific* value of $\langle \omega_1 \rangle_R = \langle \omega_2 \rangle_R = \langle \omega_3 \rangle_R$ and *vice*

versa—which undoubtedly indicates that there is no *hierarchy* between the FE and AFD motions.

BFO thus exhibits a striking type of transition that (1) possesses several OPs (i.e., $\langle u_1 \rangle$, $\langle u_2 \rangle$, $\langle u_3 \rangle$, $\langle \omega_1 \rangle_R$, and $\langle \omega_2 \rangle_R$) *with none of them being primary or more important than the other*[27] and (2) is solely driven by the collaborative *coupling* between these OPs in the low-temperature "channel" (i.e., within a rhombohedral phase). Moreover, the mutual exclusion of FE and AFD degrees of freedom in the high-temperature channel (that is within the tetragonal symmetry) provides a successful explanation of why the FE transition of BFO is of first order with no group-subgroup relation between the paraelectric and polar phases and why the Raman spectra completely disappears above T_C—as experimentally found in Refs. 9 and 11. In fact, such kind of transition exhibits all the macroscopic characteristics of the so-called "trigger-type" phase transition introduced by Holakovsky 36 years ago[20] and which is extremely rare in nature.[28,29] For instance, trigger-type phase transitions have been predicted to possess dielectric constants that follow Curie-Weiss law below T_C (Ref. 20) [unlike in improper FEs (Ref. 14)] while dramatically deviating from such law above T_C (Ref. 20) [as in improper FEs (Ref. 14)], as consistent with Fig. 1(c). Note that, on a phenomenological point of view, trigger-type transitions are characterized by a coupling between the *square* of the different OPs (including polarization) in the free-energy expansion,[20] while such coupling is *linear* in polarization and quadratic in the other OP(s) in improper FEs.[14] Note also that the original article devoted to trigger-type transitions[20] assumes that one OP is primary while the other parameter is only secondary. On the other hand, our investigated phase transition in BFO does not have any OP being primary or more important than the other.[27] We can therefore state that we discovered a special, overlooked trigger-type transition. We are thus confident that our work increases the knowledge of the broad, fascinating topic of phase transition, in addition to being of relevance to the fascinating field of multiferroics.

We acknowledge support from NOR under Grants No. N00014-04-1-0413 and No. N00014-08-1-0915; NSF under Grants No. DMR-0701558, No. DMR-0404335, and No. DMR-0080054 (C-SPIN); and DOE under Grant No. DE-FG02-05ER46188.

[1] G. A. Smolenskii and I. E. Chupis, Sov. Phys. Usp. **25**, 475 (1982).
[2] J. Wang, J. B. Neaton, H. Zheng, V. Nagarajan, S. B. Ogale, B. Liu, D. Viehland, V. Vaithyanathan, D. G. Schlom, U. V. Waghmare, N. A. Spaldin, K. M. Rabe, M. Wuttig, and R. Ramesh, Science **299**, 1719 (2003).
[3] M. Bibes and A. Barthélémy, Nature Mater. **7**, 425 (2008).
[4] A. M. Kadomtseva, Yu. F. Popov, A. P. Pyatakov, G. P. Vorob'ev, A. K. Zvezdin, and D. Viehland, Phase Transitions **79**, 1019 (2006).
[5] S. V. Kiselev, R. P. Ozerov, and G. S. Zhlanov, Sov. Phys. Dokl. **7**, 742 (1963); G. A. Smolenskii, V. Isupov, A. Agranovskaya, and N. Krainik, Sov. Phys. Solid State **2**, 2651 (1961).
[6] J. R. Teague, R. Gerson, and W. J. James, Solid State Commun. **8**, 1073 (1970).
[7] I. Sosnowska, M. Lowenhaupt, W. I. F. David, and M. R. Ibberson, Physica B **180-181**, 117 (1992).
[8] P. Fischer, M. Polomska, I. Sosnowska, and M. Szymanski, J. Phys. C **13**, 1931 (1980).
[9] R. Haumont, J. Kreisel, P. Bouvier, and F. Hippert, Phys. Rev. B **73**, 132101 (2006).
[10] C. Kittel, *Introduction to Solid State Physics*, 7th ed. (Wiley, New York, 1996).
[11] I. A. Kornev, S. Lisenkov, R. Haumont, B. Dkhil, and L. Bellaiche, Phys. Rev. Lett. **99**, 227602 (2007).
[12] S. Kamba, D. Nuzhnyy, M. Savinov, J. Sebek, J. Petzelt, J. Prokleska, R. Haumont, and J. Kreisel, Phys. Rev. B **75**, 024403 (2007).
[13] B. J. Campbell, H. T. Stokes, D. E. Tanner, and D. M. Hatch, J. Appl. Crystallogr. **39**, 607 (2006).
[14] A. P. Levanyuk and D. G. Sannikov, Sov. Phys. Usp. **17**, 199 (1974).
[15] T. Kimura, T. Goto, H. Shintani, K. Ishizaka, T. Arima, and Y. Tokura, Nature (London) **426**, 55 (2003).
[16] L. Dai and Q. Jiang, J. Appl. Phys. **101**, 064117 (2007).
[17] A. Malashevich and D. Vanderbilt, Phys. Rev. Lett. **101**, 037210 (2008).
[18] H. T. Stokes, C. Sadate, D. M. Hatch, L. L. Boyer, and M. J. Mehl, Phys. Rev. B **65**, 064105 (2002).
[19] Therefore, BFO does not fall into the category of materials that are addressed in Ref. 13 and that exhibit multiple, rather than none primary OPs, each belonging to a single irreducible representation.
[20] J. Holakovský, Phys. Status Solidi B **56**, 615 (1973).
[21] W. Zhong, D. Vanderbilt, and K. M. Rabe, Phys. Rev. Lett. **73**, 1861 (1994); Phys. Rev. B **52**, 6301 (1995).
[22] I. A. Kornev, L. Bellaiche, P. E. Janolin, B. Dkhil, and E. Suard, Phys. Rev. Lett. **97**, 157601 (2006).
[23] A. García and D. Vanderbilt, Appl. Phys. Lett. **72**, 2981 (1998).
[24] K. M. Rabe and E. Cockayne, in *First-Principles Calculations for Ferroelectrics: Fifth Williamsburg Workshop*, edited by R. E. Cohen (AIP, Woodbury, New York, 1998), p. 61.
[25] *Phase Transitions and Critical Phenomena I–V*, edited by C. Domb and M. S. Green (Academic, New York, 1972).
[26] Similarly, FE and AFD motions do not want to coexist in an orthorhombic phase in which **u** would be parallel to the $\langle 001 \rangle$ direction and $\boldsymbol{\omega}_{\mathbf{R}}$ would lie along *another* $\langle 001 \rangle$ direction (being perpendicular to **u**) because of the positive, large D_{xxyy}.
[27] Alternatively, one can also consider that this unusual phase transition has a multicomponent primary OP, that is ($\langle u_1 \rangle$, $\langle u_2 \rangle$, $\langle u_3 \rangle$, $\langle \omega_1 \rangle_R$, and $\langle \omega_2 \rangle_R$), involving *two* different irreducible representations [rather than a single one as assumed in the conventional Landau theory (Ref. 14)].
[28] M. Bonin, A. Fuith, K. J. Schenk, and P. Tolédano, Phys. Rev. B **59**, 14246 (1999).
[29] As shown in J. Iniguez, S. Ivantchev, J. M. Perez-Mato, and A. Garcia, Phys. Rev. B **63**, 144103 (2001), the *free energy* associated with the effective Hamiltonian can have sextic terms, as consistent with the model developed by Holakovsky (Ref. 20).